Fine-Tuning the Design: Practical Application of Discrete Fracture Networks in 3D Finite-Element Models

*Gordon Sweby[1], Rebecca Carlton[2] and John Player[1]

[1] MineGeotech P/L, Perth, Australia (*gordonsweby@minegeotech.com.au & johnplayer@minegeotech.com.au)
[2] Bellevue Gold Ltd, Perth, Australia (rcarlton@bgl.gold)

Abstract. Application of discrete fracture networks (DFN) for detailed analysis of operational mine designs is demonstrated by means of two case studies. The first case is an open pit where a section of the pit design was re-analysed using a DFN to provide confirmation of the applicability of the slope design parameters. The second case involves the proposed stoping of an ore block located below a critical piece of mine infrastructure and confirmation of its stability was a key requirement to proceed. In both cases the internal DFN generator tool in RS3 was used. Both cases provided defendable results on which to base operational decisions, to a higher level of confidence than conventional analysis methods involving semi-empiricism (rockmass strength approach).

Keywords: Discrete Fracture Network, mine design, three-dimensional analysis, finite-element, stope, pillar

1 Introduction

This paper discusses the application of Discrete-Fracture-Networks (DFN) for detailed analysis of specific mine design issues, where it is deemed that conventional semi-empirical methods are inadequate to provide the required level of confidence. Two case studies are presented, using RS3, which attempt to achieve that aim.

The first is an open pit where conventional Hoek-Brown strength downrated by Geological Strength Index had been applied for overall slope stability analysis. A section of wall was re-analysed using a DFN representation to investigate potential implications (Figure 1).

The second case study involved the proposed stoping of an ore block below a critical piece of mine infrastructure (decline) that required stability over the mine life (Figure 2).

The DFN approach aims to simulate a fractured rock mass by explicitly modelling joints in a network. The DFN networks generated in these examples are based on statistical data inputs from mapping or logging of joints.

R. Hammah et al. (eds.), *Proceedings of the Rocscience International Conference 2025 (RIC 2025)*, Atlantis Highlights in Engineering 40,
https://doi.org/10.2991/978-94-6463-900-1_2

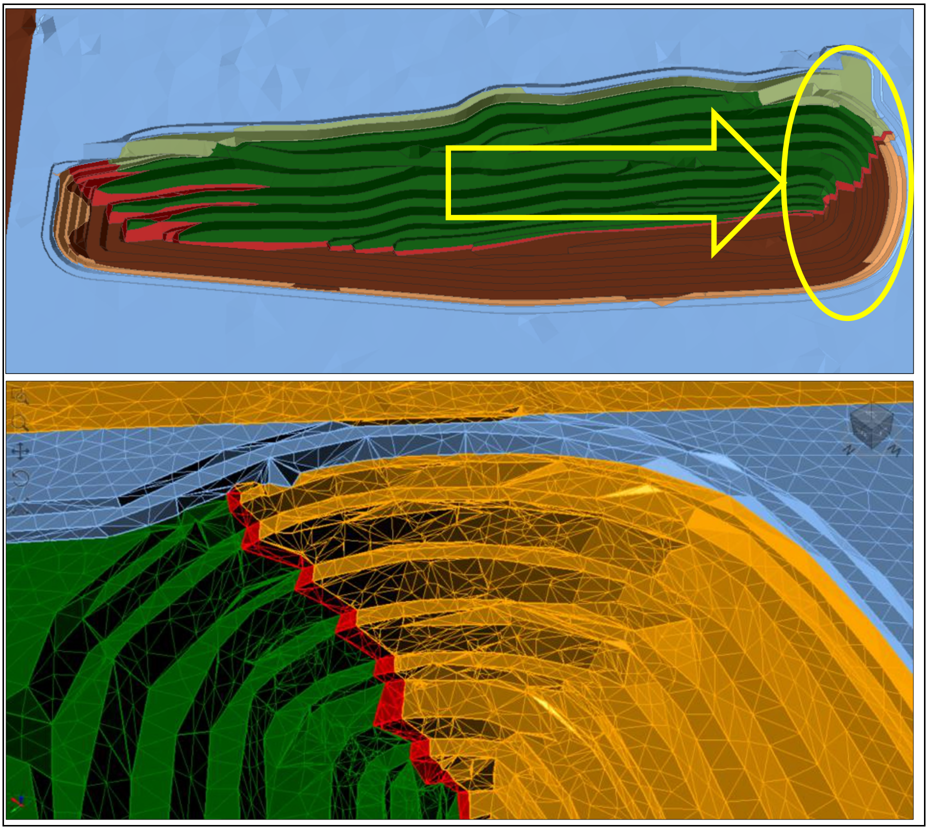

Figure 1 Case Study 1 - Section of pit endwall selected for detailed design

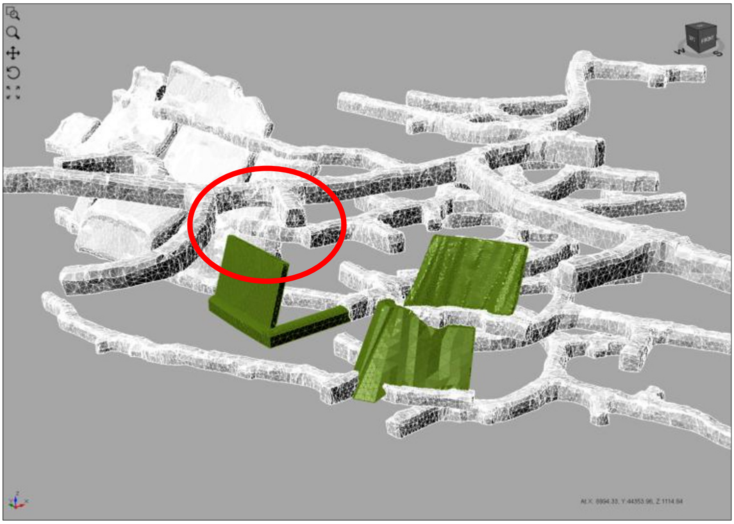

Figure 2 Case Study 2 - Proposed stoping below key infrastructure (decline) in circled area

2 Local Geology and Geotechnical Assumptions

2.1 Case Study 1

The pitwalls are comprised of mafic/ultramafic, extrusive and volcaniclastic rocks of Archaean age. The mineralisation is vanadiferous titanomagnetite hosted within an intrusive gabbro complex.

Three main geotechnical domains have been defined for the purposes of design, namely;

- Footwall gabbro
- Hangingwall gabbro
- Schist

Fresh and transitional weathered subdomains have been modelled, as well as a thin saprolite (soil-like) surface layer. A section through the RS3 finite-element model is shown in Figure 3.

Model input strength parameters for the design domains are as given in Table 1.

No stress measurement data is available at this site, so the far-field stress tensor given in Table 2 has been assumed, based on measurements at nearby sites.

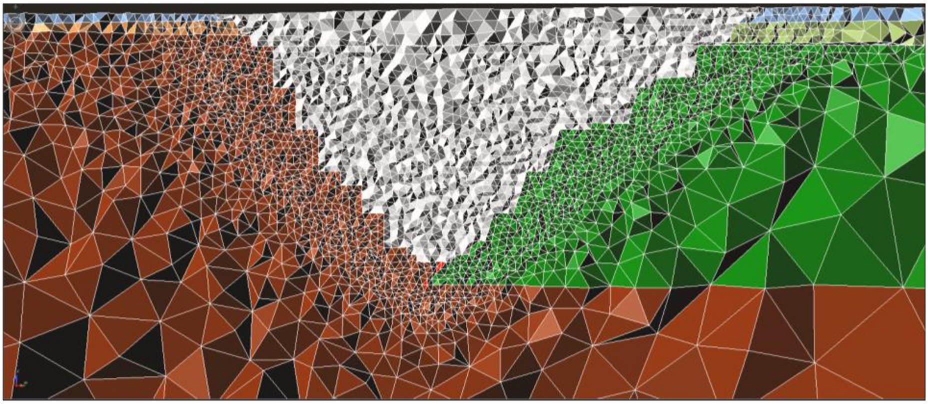

Figure 3 Section through RS3 model showing design domains and mesh discretisation

Table 1 Rock mass strength input parameters for the modelled design domains

Geotechnical Design Domain	Geological Strength Index (GSI)	Hoek-Brown Sc	Hoek-Brown mi	Density (t/m^3)	Modulus (GPa)	Cohesion (MPa)	Friction Angle
Transitional Hangingwall	37	90	20.0	2.96	16	n/a	n/a
Transitional Footwall	50	n/a	n/a	n/a	n/a	n/a	n/a
Transitional Schist	49	18.5	16.5	2.71	3.5	n/a	n/a
Fresh Hangingwall	67	170	14	3.07	31	n/a	n/a
Fresh Footwall	72	125	9.0	2.75	23	n/a	n/a
Fresh Schist	60	90	9.5	2.9	16.5	6.2	39

Table 2 Assumed far-field stress, based on measurements at nearby mines

Principal Stress	k-ratio	Azimuth	Dip
Maximum	2.5	065	00
Intermediate	1.5	155	00
Minimum	n/a	000	90

Joint orientation and spacing data have been acquired during the study investigations, by means of acoustic televiewer (ATV) downhole surveys, and the summary results shown in Figure 4. Four dominant sets have been identified and summarised in Table 3.

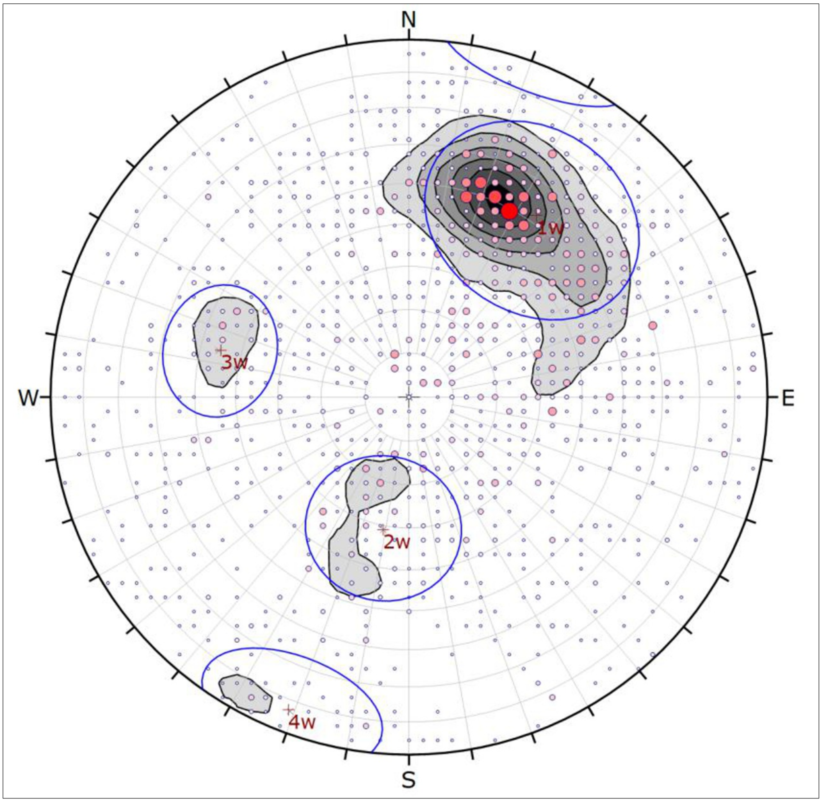

Figure 4 Stereographic projection of ATV measured joints and identified sets

Table 3 Identified joint sets, orientation and spacing

Defect Set	Azimuth (°)	Dip (°)	Spacing (m)
1	215	52	3.1
2	011	31	6.9
3	104	45	5.0
4	021	83	6.1

2.2 Case Study 2

The model geometry is hosted entirely in archaean basalt, with gold mineralisation hosted in foliated quartz veins. The model input strength parameters for these design domains are as given in Table 4.

Table 4 Rock mass strength input parameters for the modelled design domains

Geotechnical Design Domain	Geological Strength Index (GSI)	Hoek-Brown Sc	Hoek-Brown mi	Density (t/m^3)	Modulus (GPa)
Basalt	80	310	12	3.01	48
Vein Quartz	88	145	12	2.91	25.5

The far-field stress assumption is based on acoustic emission (AE) measurements carried out on oriented exploration core, with verification by means of core discing and borehole breakout observations (Table 5).

Table 5 Assumed far-field stress

Principal Stress	k-ratio	Azimuth	Dip
Maximum	2	040	00
Intermediate	1.5	130	00
Minimum	n/a	000	90

Joint data has been provided in the form of line mapping in development sited within the volume of interest, an example of which is shown in Figure 5. A stereographic projection showing the distribution of mapped structure is shown in Figure 6.

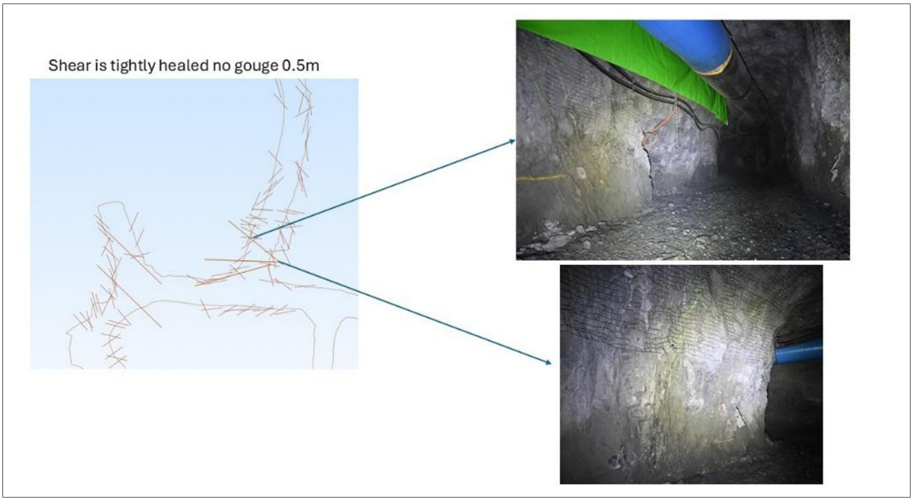

Figure 5 Scanline mapping of joints and major structures occurring in the volume of interest

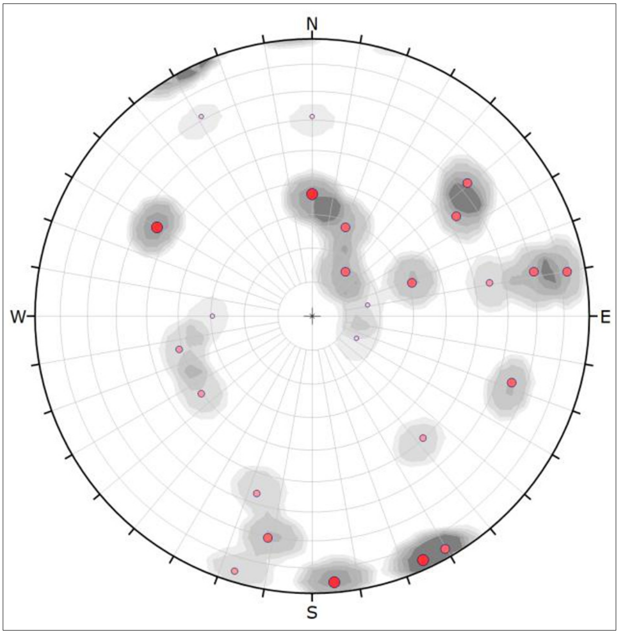

Figure 6 Stereographic projection of mapped joints

3 Discrete Fracture Network Generation

The internal RS3 DFN generator tool was used in both case studies. This tool allows for stochastic inputs for spacing, length and persistence, but not orientation. The respective DFN's generated in each case are shown in Figure 7 and Figure 8.

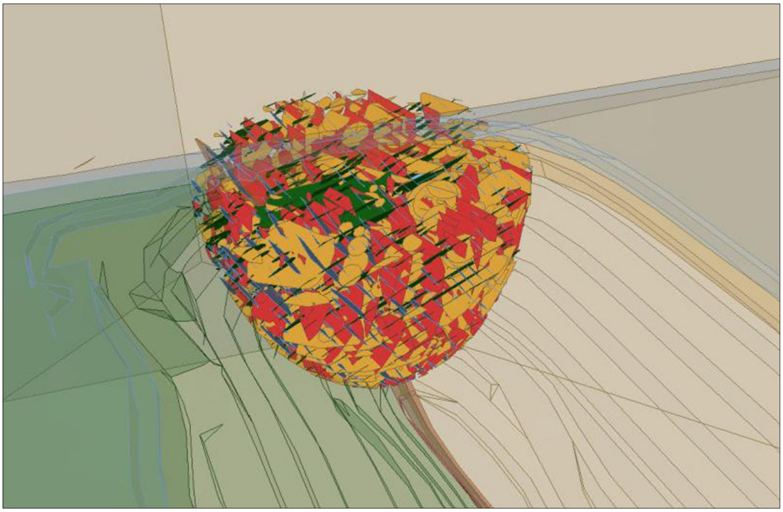

Figure 7 Parallel DFN generated for Case Study 1

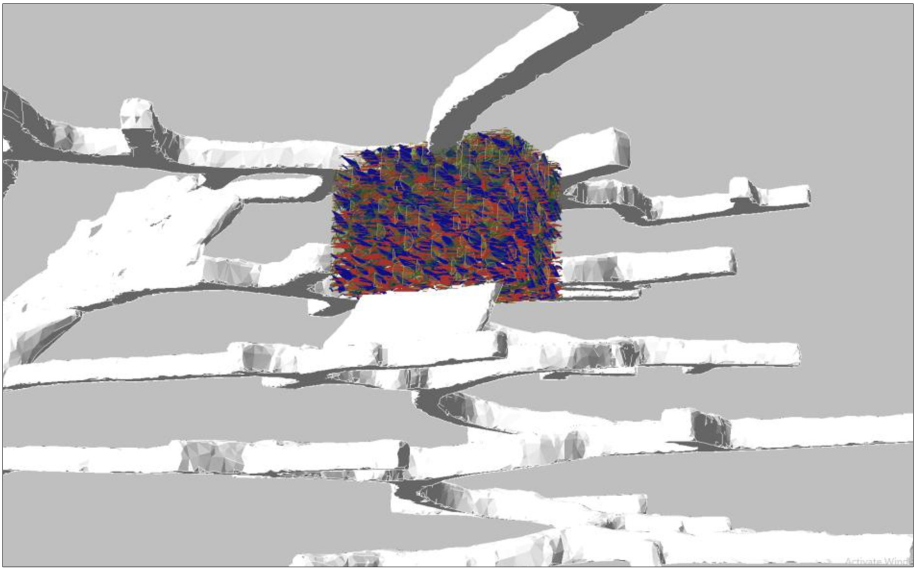

Figure 8 Parallel DFN generated for Case Study 2

4 Modelling Goals and Strategy

4.1 Case Study 1

For the open pit, the primary goal of the modelling was to verify that the Strength Reduction Factor (SRF) of the SE endwall met the design acceptance criterion of 1.5 (for a low confidence geotechnical model and low failure consequence). The GSI analysis carried out previously had determined the SRF (Factor-of-Safety) to be 5.5.

4.2 Case Study 2

For the case where a stope was to be mined below critical infrastructure, the goal was to verify that the pillar between the stope crown and the decline has a SRF in excess of 2.0. This assessment criterion was agreed to after discussion with the Client and deemed adequate for long term stability.

5 Results

5.1 Case Study 1

Stability analysis resulted in a critical SRF of 3.4, which is less than the SRF obtained by GSI analysis, but sufficient to satisfy the design acceptance criterion of 1.5. The extent of potential instability is shown by means of a displacement isosurface. Slip on modelled defects is shown by means of plastic shear strain contours in Figure 10. From this it is clear that the local instability volume is being influenced by both intact rock yield and joint slip, thus a more accurate representation of the failure mechanism likely to influence the slope. A deformed surface contour (Figure 11) further aids the interpretation of the mechanism.

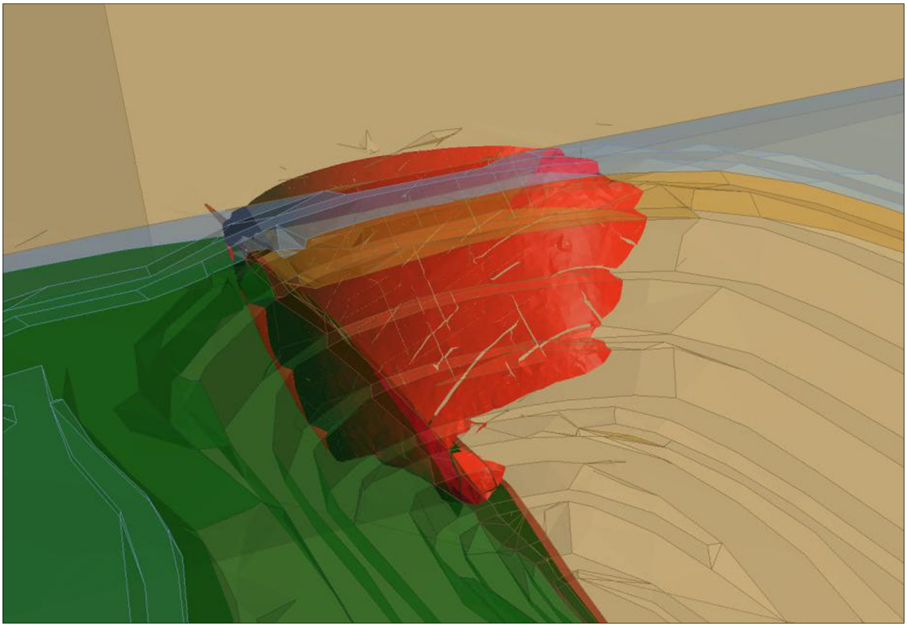

Figure 9 Isosurface defining extent of potential instability (at a SRF of 3.45)

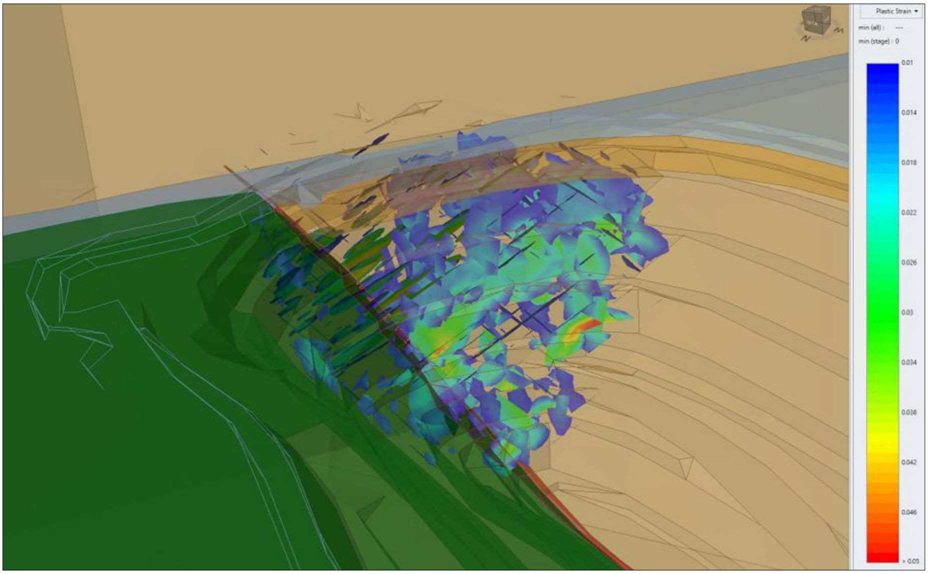

Figure 10 Plastic shear strain on modelled defects (indicating slip)

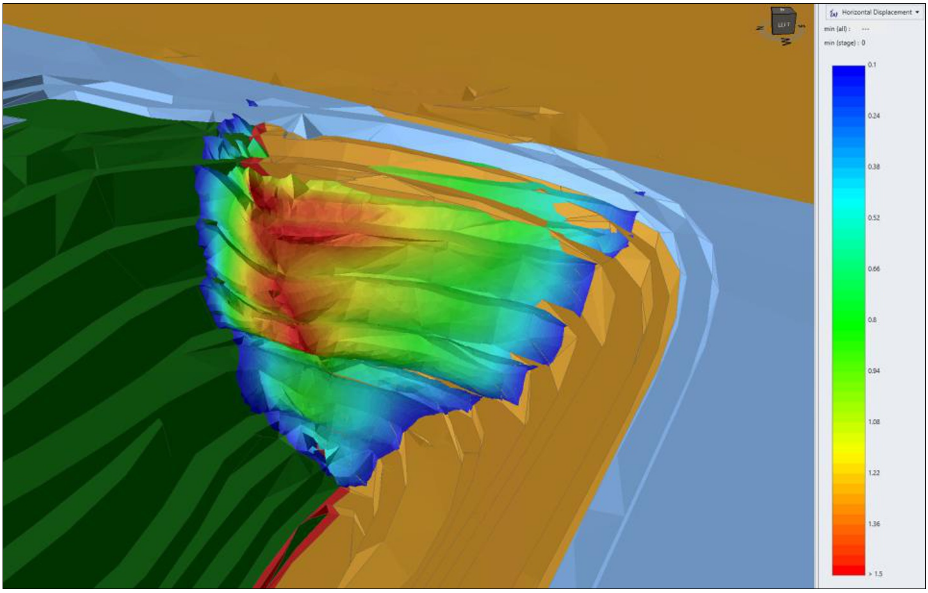

Figure 11 Deformed displacement contours showing the sense of movement of the unstable material (at a SRF of 3.5)

5.2 Case Study 2

The pillar between the stope crown and the decline was found to be stable at a SRF of 1.0 and at a SRF of 2.0, thus satisfying the design acceptance criterion. Isosurfaces representing damage (volumetric strain) are shown in Figure 12 and Figure 13 and there is negligible difference between the two. Figure 14 and Figure 15 show the increase in defect slip between a SRF of 1.0 and a SRF of 2.0. This is the effect of halving the joint shear strength and does not impact the overall stability of the pillar.

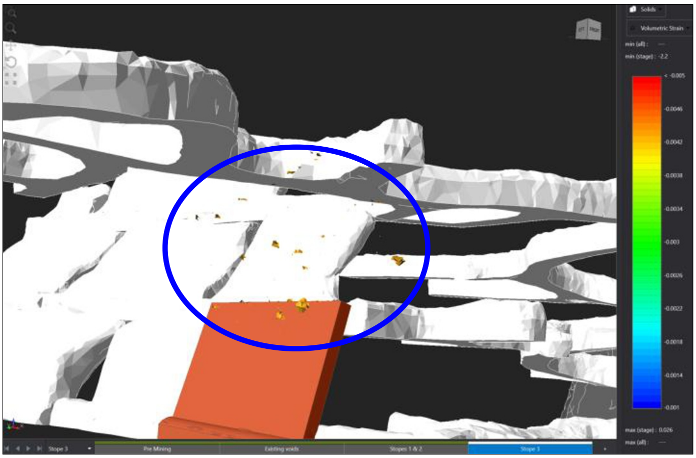

Figure 12 Isosurfaces (orange) representing damage (cracking) at a SRF of 1.0

Figure 13 Isosurfaces (orange) representing damage (cracking) at a SRF of 2.0

Figure 14Joint plastic shear strain (slip) at a SRF of 1.0

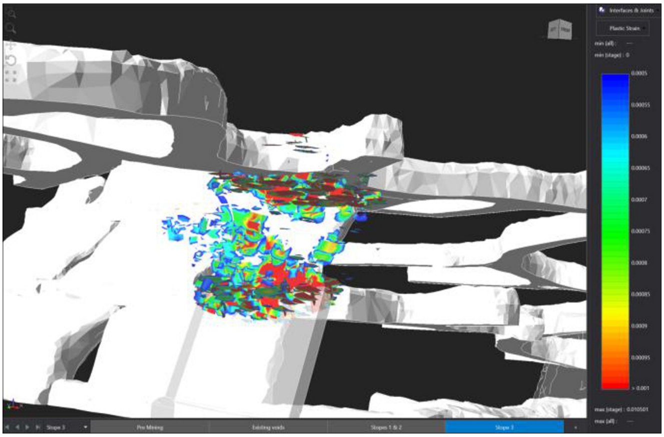

Figure 15 Joint plastic shear strain (slip) at a SRF of 2.0

6 Conclusions

Two case studies are presented which demonstrate the use of discrete-fracture-networks for detailed analysis of specific and critical design issues.
In each case, high-confidence structural data was available and thus the approach is justified and an alternative to the conventional Hoek-Brown strength criterion with GSI downrating.
However significant unknowns still exist, for example the length and persistence of structural data where only core or ATV data is available. In these cases, it would be ideal to perform sensitivity analysis using the stochastic inputs available in RS3 (time and budget permitting).

References

1. Rocscience Incorporated: RS3v4.036 3D finite element analysis program for modelling slopes, tunnel and support design, surface and underground excavations. Rocscience, Ont, Canada